Society For Biomaterials

# Award Winner in the Young Investigator Category, 2017 Society for Biomaterials Annual Meeting and Exposition, Minneapolis, MN, April 05–08, 2017

## Lymph node stiffness-mimicking hydrogels regulate human B-cell lymphoma growth and cell surface receptor expression in a molecular subtype-specific manner

**F.N.U. Apoorva,[1] Ye F. Tian,[1] Timothy M. Pierpont,[2] David M. Bassen,[3] Leandro Cerchietti,[4] Jonathan T. Butcher,[3] Robert S. Weiss,[2] Ankur Singh[1,3*]**

[1]Sibley School of Mechanical and Aerospace Engineering, College of Engineering, Cornell University, Ithaca, New York
[2]Department of Biomedical Sciences, College of Veterinary Medicine, Cornell University, Ithaca, New York
[3]Meinig School of Biomedical Engineering, College of Engineering, Cornell University, Ithaca, New York
[4]Division of Hematology and Medical Oncology, Weill Cornell Medical College of Cornell University, New York, New York

Received 17 October 2016; revised 16 December 2016; accepted 10 January 2017
Published online 12 April 2017 in Wiley Online Library (wileyonlinelibrary.com). DOI: 10.1002/jbm.a.36031

**Abstract:** Diffuse large B-cell lymphoma (DLBCL) is the most common type of non-Hodgkin's lymphoma, with multiple molecular subtypes. The activated B-cell-like DLBCL subtype accounts for roughly one-third of all the cases and has an inferior prognosis. There is a need to develop better class of therapeutics that could target molecular pathways in resistant DLBCLs; however, this requires DLBCLs to be studied in representative tumor microenvironments. The pathogenesis and progression of lymphoma has been mostly studied from the point of view of genetic alterations and intracellular pathway dysregulation. By comparison, the importance of lymphoma microenvironment in which these malignant cells arise and reside has not been studied in as much detail. We have recently elucidated the role of integrin signaling in lymphomas and demonstrated that inhibition of integrin-ligand interactions abrogated the proliferation of malignant cells *in vitro* and in patient-derived xenograft. Here we demonstrate the role of lymph node tissue stiffness on DLBCL in a B-cell molecular subtype specific manner. We engineered tunable bioartificial hydrogels that mimicked the stiffness of healthy and neoplastic lymph nodes of a transgenic mouse model and primary human lymphoma tumors. Our results demonstrate that molecularly diverse DLBCLs grow differentially in soft and high stiffness microenvironments, which further modulates the integrin and B-cell receptor expression level as well as response to therapeutics. We anticipate that our findings will be broadly useful to study lymphoma biology and discover new class of therapeutics that target B-cell tumors in physical environments. © 2017 Wiley Periodicals, Inc. J Biomed Mater Res Part A: 105A: 1833–1844, 2017.

**Key Words:** B-cell receptor, organoids, integrin, germinal center, tissue stiffness, biomechanics, extracellular matrix, chemoresistance, contractility, DLBCL

**How to cite this article**: Apoorva FNU, Tian YF, Pierpont TM, Bassen DM, Cerchietti L, Butcher JT, Weiss RS, Singh A. 2017. Lymph node stiffness-mimicking hydrogels regulate human B-cell lymphoma growth and cell surface receptor expression in a molecular subtype-specific manner. J Biomed Mater Res Part A 2017:105A:1833–1844.

### INTRODUCTION

Despite advances in therapeutics and diagnostics, many mature B-cell lymphomas remain incurable. This is partly attributable to the genetic heterogeneity of B-cell lymphomas as well as the complex growth and survival signaling provided by the biophysical, biochemical, and cellular components of the lymphoid tumor microenvironment. Diffuse large B-cell lymphoma (DLBCL) is the most common lymphoma, representing ~30–40% of all B-cell non-Hodgkin's lymphomas, and gene expression profiling has allowed sub-classification into germinal center B cell (GCB) and activated B-cell (ABC) DLBCL subtypes.[1–6] The standard combination chemotherapy, CHOP (cyclophosphamide, doxorubicin, vincristine, prednisone) was the frontline therapy for many years, until the addition of Ritxumab (R-CHOP). Still, a significant percentage of DLBCL patients are

*Correspondence to: A. Singh; e-mail: as2833@cornell.edu
Contract grant sponsor: National Cancer Institute; contract grant number: 1R21CA185236-01 (AS) and R01CA163255-05 (RSW)

not cured. Activated B-cell-like (ABC) DLBCL is the most chemo-resistant DLBCL subtype with poor 5-year overall survival compared to germinal center B-cell-like (GCB) DLBCL.[2,7,8] Improved therapies are needed for all DLBCLs but most urgently for ABC-DLBCLs. A myriad of predictive biomarkers for resistance have been identified, including genetic and proteomic signature, stromal signatures, and somatic mutations.[7,9] But none is sufficient to predict resistance in a given patient and few are helpful in guiding selection of targeted therapies. Therefore, new treatments and treatment-specific biomarkers are needed to improve clinical outcome of both ABC and GCB DLBCL patients. However, rational clinical translation requires understanding the factors that modulate expression level of BCR in lymphomas.

The microenvironment in tumors often differs from that in normal tissue, exhibiting altered composition and density of ECM proteins, stromal and immune cells, and growth factors. This altered microenvironment has been implicated as contributing to cancer development and progression for a variety of tumors.[10–12] However, the role of the lymphoid tumor microenvironment, where lymphomas arise and reside, remains unclear. A major bottleneck in the field is that it remains unclear how combinations of biophysical and/or biomolecular signals that exist in close spatial and temporal order across the lymphoma tumor microenvironment affect ABC-DLBCL and GCB-DLBCL growth and response to therapies. The tumor microenvironment of B-cell lymphomas contains highly variable numbers of immune cells, stromal cells, blood vessels and an altered extracellular matrix.[13] In the recent years, we and others have shown that the crosstalk between lymphoma cells and the extracellular matrix via integrin molecules is important for their survival and chemoresistance.[14–16] Specifically, in our effort to understand the role of lymphoma microenvironment, we have recently shown that the crosstalk between the lymphoma microenvironment and integrin $\alpha v\beta 3$ is critical for human T-cell lymphoma survival, both *in vitro* and *in vivo*.[16] In contrast, we discovered that human ABC-DLBCLs have a differential need for integrin $\alpha 4\beta 1$ and $\alpha v\beta 3$ for survival,[17] in a stromal follicular dendritic cell-dependent manner. We now hypothesize that extracellular matrix stiffness is another aspect of the lymph node biophysical microenvironment that can influence lymphoma fate.

For many cancers, increased extracellular matrix stiffness is associated with induction and progression of malignant phenotypes.[10,18] In line with these observations and others, several bioengineered scaffolds have been developed to study the role of mechanical stiffness in tumor survival and progression. A recent study evaluated the role of 3D matrix stiffness on proliferation and drug sensitivity of human myeloid leukemia, which represent liquid tumors originating from bone marrow.[19] However, to date, there are no reported studies on the role of tissue stiffness in lymphomas which arise and for the most part, reside in lymphoid tissues such as lymph nodes. Despite the enlargement and palpable stiffness of neoplastic lymphoid tissue typically used as an initial screen, the role of lymphoid tissue stiffness in lymphoma remains unclear. The challenge in performing these studies is lack of tunable *ex vivo* engineered systems that present survival signals to lymphomas and limited understanding of lymphoid tissue stiffness.

Here we quantify healthy and neoplastic lymph node (and spleen) tissue biomechanics using micropipette aspiration. This technique measures local tissue distention due to applied vacuum pressure, analogous to a uniaxial tensile test, as demonstrated by us using finite element analysis.[20,21] We demonstrate that lymphoid tumors have increased tissue stiffness as compared to healthy lymph nodes and spleen. We correlated this data with independent rheology measurements, and engineered hydrogel-based organoids with physiological or pathologically stiff matrix. We demonstrate design of biomaterials-based hydrogels with tunable mechanical stiffness for growth modulation of B-cell lymphomas, and discover that lymphomas respond differentially to soft and high stiffness microenvironments in a molecular subtype dependent manner. Engineered hydrogel-based lymphoma organoids using our previously reported immune organoids[22,23] demonstrate that lymphoid-mimicking stiffness can act as an important biophysical stimulus on lymphoid tumor cells by influencing BCR and integrin expression levels, with consequences on cell survival and drug resistance, depending on the particular DLBCL molecular subtype. This is the first study, to our knowledge, that demonstrates the role of lymphoid tissue stiffness on the prosurvival surface receptors and drug response in genetically diverse B-cell lymphomas.

## MATERIALS AND METHODS

### Tg(IghMyc)22Bri (*E*μ-*myc*) mouse model of human lymphoma

Tg(IghMyc)22Bri (*E*μ-*myc*) mice on the C57BL/6J strain background were purchased from the Jackson Laboratory and maintained as hemizygotes. All animals used in this study were handled in accordance with federal and institutional guidelines, under a protocol approved by the Cornell University Institutional Animal Care and Use Committee (IACUC). Mice were monitored regularly and sacrificed upon reaching humane endpoint criteria.

### Human B- and T-cell lymphoma lines

Lymphoma cell lines that represent a spectrum of DLBCL were used in the current study. These cell lines included: HBL-1 (ABC-DLBCL, IgM BCR dependent), LY-10 (ABC-DLBCL, IgM BCR dependent), LY-3 (ABC-DLBCL, IgM BCR independent), and LY-1 (GCB-DLBCL, IgM BCR independent). Human tonsil derived follicular dendritic cells (FDC) were used as supporting stromal cells for human lymphomas.[17] All cells except LY-10 were cultured in RPMI 1640 media supplemented with 10% fetal bovine serum and 1% penicillin/streptomycin. LY-10 cells were cultured in Iscove's Modified Dulbecco's media (IMDM) supplemented with 20% fetal bovine serum and 1% penicillin/streptomycin. The subsequent passage of these lymphoma cells involved use of 20% conditioned media from previous culture.[17] Deidentified, freshly isolated primary human follicular B-cell lymphoma tissue from lymph node of an untreated patient was made available by Dr. Leandro Cerchietti at Weill Cornell Medical College of Cornell University, in accordance with the Institutional Review Board guidelines.

### Hydrogel fabrication and mechanical testing

A stock solution of 6% (weight/volume) gelatin (Sigma-Aldrich) in RPMI or IMDM media and stock suspension of 4% silicate nanoparticles (diameter ~25 nm and thickness ~1 nm; Southern Clay Products Inc.) was freshly prepared in sterile deionized water. We have previously shown that mixing gelatin and silicate nanoparticles results in the formation of a stable hydrogel network.[22,23] Lymphoma cells (12,000 per 12 μL hydrogel) with and without FDCs (6000 per 12 μL hydrogel) were added to gelatin stock solution. The FDCs were mitotically inhibited through incubation in cell culture medium containing 0.01 mg/mL Mitomycin C at 37°C for 45 min in complete media conditions prior to the encapsulation. The cells were rinsed twice with 10 mL of 1× PBS before usage in the experiments. The two stock solutions were mixed together using the repeated pipetting method, as described earlier by us,[22,23] to achieve a cross-linked 12 μL hydrogel organoids with (a) 2% gelatin and 2% nanoparticle, (b) 2.5% gelatin and 2% nanoparticle, and (c) 3% gelatin and 2% nanoparticle compositions. Organoids were fabricated in non-treated 96-well plates, cured for 5 min before adding growth media, which was replaced every 3 days. For stiffness measurements (storage modulus), hydrogels were analyzed using a Paar Physica MCR 300 rheometer with 50 mm flat-plate geometry under a strain sweep (1–10% strain) condition at a fixed frequency of 0.1 Hz and temperature of 37°C.

### Micropipette aspiration method to determine soft tissue stiffness

Lymphoid tissue and hydrogel mechanical properties were quantified using our well characterized micropipette aspiration method.[20,21,24] Isolated murine or primary human tissues or hydrogels were placed directly in phosphate-buffered saline (PBS) and a drawn glass capillary micropipette ($r_p \geq 35$ μm) was placed adjacent to the sample surface. Vacuum pressure was incrementally applied via silicone tubing and calibrated by manometer. Previous strain history was mitigated by preconditioning with ~20 cycles of low pressurization (<1 Pa). The lowest pressure that ensured stable contact with the micropipette was taken as zero pressure. Monotonically increasing pressure loads were then applied quasitatically, with images captured at each increment at 150× magnification using a Zeiss Discovery v20 stereo microscope (Spectra Services, Inc.). The aspirated length was measured using calibrated images in NIH ImageJ. An experimental "stretch ratio," $\lambda = (L + r_p)/r_p$ was defined by normalizing the aspirated length to the pipette radius as previously described.[20,21] The $\Delta P$ versus $\lambda$ curves were fit using the axial Cauchy stress for a uniaxial load of an incompressible material with an assumed exponential material law, specifically,

$$\sigma_{yy} = \alpha C \exp\left[\alpha\left(\lambda^2 + \frac{2}{\lambda} - 3\right)\right]\left(\lambda^2 - \frac{1}{\lambda}\right) \quad (1)$$

The fitting parameters $\alpha$ and $C$ were determined by minimizing the sum of the errors squared between Eq. (1) and the $\Delta P$ versus $\lambda$ data curves. The $C$ parameter was modified using a scale factor determined from finite element simulation, reported earlier by us, $C_{mod} = \gamma(\alpha)C$.[20] Strain energy density was evaluated as a metric for comparing mechanical testing data as previously described.[20,21] Data was presented with representative stress response curves and strain energy density values were presented as mean ± SEM with $n = 3$. Statistical comparisons were performed using ANOVA with Tukey post-tests or Student's $t$ test, $^*p < 0.05$.

### Cellular analyses of lymphomas in organoids

Lymphoma proliferation studies were performed using a CellTiter 96 AQueous One Solution Cell Proliferation Assay (Promega), as reported earlier by us.[17,25,26] Typically, on days 1, 3, and 5, media was removed and organoids were washed once with PBS. CellTiter reagent was added as per manufacturer's recommendation, and analyzed after 4 hours using a Biotek H1 Hybrid plate reader. For flow cytometry analysis, cells were harvested from organoids by means of enzymatic degradation with a collagenase solution (25 U/mL; Worthington Biosciences) for 6 hours. The degraded organoid suspension was passed through a 70 μm filter (BD Falcon) to separate the cells from any polymeric debris. The harvested cells were washed twice to remove the remaining collagenase and stained with antibodies against B-cell marker CD19, BCR IgM, integrins CD29 (β1) and CD49D (α4) at 1:500 dilutions for 1 hour at 4°C. The antibodies used for flow cytometry studies were Anti Human IgM (APC), Anti Human CD20 (FITC), Anti Human CD19 (FITC), Anti Human CD49D (APC), and Anti Human CD29 (APC), and all were purchased from eBiosciences. The stained cells were washed twice, resuspended in equal volume of FACS buffer and analyzed using a BD Accuri C6 flow cytometer. FlowJo software was used to analyze data. For the Rho-ROCK pathway inhibition studies, lymphoma organoids were cultured in 1 n$M$ Y-27632 reconstituted lymphoma growth media for 48 hours, followed by proliferation analysis.

### Drug-induced apoptosis studies in organoids

All drug studies were performed by allowing cells to proliferate in organoids with varying stiffness or 2D cultures for 3 days under normal growth conditions followed by addition of the therapeutics. We studied two classes of drugs: a conventional chemotherapeutic vincristine (0.5 μ$M$), which inhibits microtubule polymerization, and Panobistant (50 n$M$), a Histone Deacetylase Inhibitor (HDACi). After 48 hours of drug exposure, cells were harvested and stained with Annexin V-FITC (Biotium) and CD19 B-cell markers. Stained cells were quantified for percent apoptosis using Accuri C6 flow cytometer (BD Biosciences) and analyzed using FlowJo software.

### Statistical analysis

The statistical analysis of variance (Tukey's test for one-way ANOVA or Bonferroni correction for two-way ANOVA) was carried using GraphPad Prism software. A $p$ values of <0.05 was considered significant. Two tail $t$-tests were performed

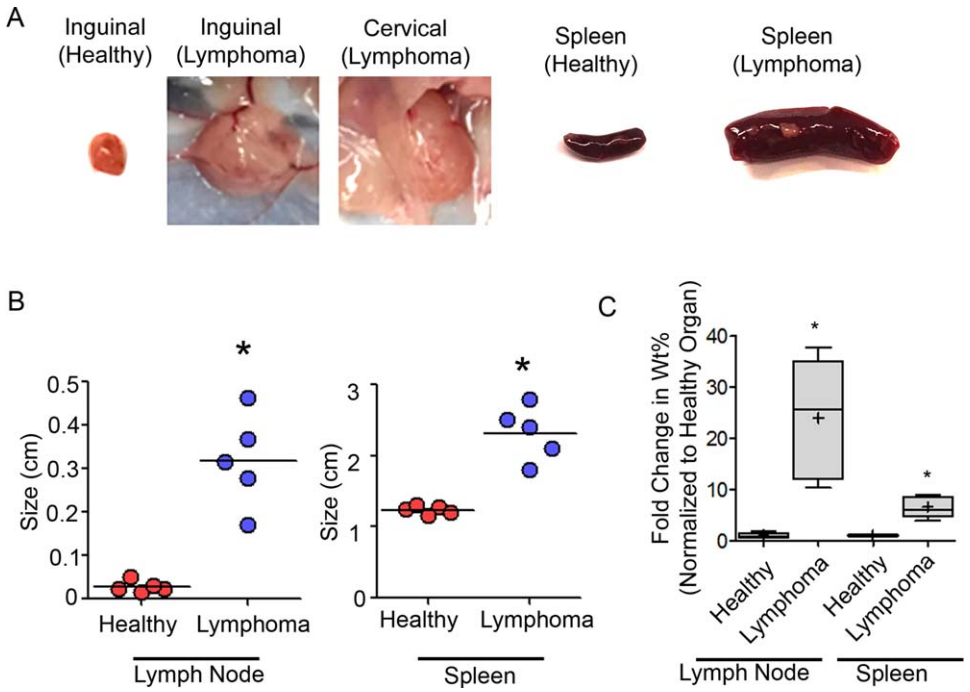


**FIGURE 1**. Change in lymph node and spleen size, and weight with lymphoma tumorigenesis. (A) Photographs representing healthy and neoplastic lymph nodes and spleen from Eμ-myc mice. Animals were sacrificed prior to showing clinical signs (healthy) or upon reaching health endpoints (lymphoma). (B) Change in the size of lymph node and spleen isolated from Eμ-myc mice pre-and-post lymphomagenesis; $N = 5$; mean ± SEM; $p < 0.05$. (C) Fold change in the weight % of lymph node and spleen isolated from Eμ-myc mice pre-and-post lymphomagenesis. Weight percentage was initially measured relative to body weight and then normalized to healthy lymph node or spleen, respectively; $N = 5$; mean ± SEM; $p < 0.05$.

for comparison between two groups. All experiments were reproduced and performed in triplicates unless otherwise mentioned. The quantities are reported in the form of mean ± SEM

## RESULTS AND DISCUSSION

### Change in physiological and mechanical properties of primary lymphoma tissues

To characterize changes in the stiffness of lymphoid tissues at the end of tumorigenesis, we first determined the change in the size of lymph nodes and spleen harvested from the Eμ-myc mouse model of human B-cell lymphoma.[27] Oncogenesis in these mice is driven by the presence of a transgene containing the c-Myc gene under the control of the immunoglobulin heavy chain enhancer (Eμ) and c-Myc promoter. In these animals, c-Myc is overexpressed in B lymphoid cells, resulting in hyperproliferation of the pre-B-cell population prenatally as well as spontaneous formation of lymphoma. Nearly all Eμ-myc mice eventually develop pre-B- or B-cell lymphomas, with approximately 50% of animals developing neoplasms by 15–20 weeks of age. As indicated in Figure 1A,B, both inguinal and cervical lymph node showed marked enlargement as compared to a healthy lymph node (~10-fold larger size; 0.3 cm with tumor-bearing mice; $p < 0.05$). Similarly, spleen, another common lymphoid tissue for lymphomagenesis, also indicated a significant increase in tissue size as compared to healthy spleen (Figure 1A,B; $p < 0.05$). We further quantified the fold change in weight percentage of these enlarged tumors and observed ~25-fold increase in lymph node weight and ~8-fold increase in spleen (Fig. 1C; $p < 0.05$).

Previously reported mechanical properties of lymph node and spleen are technique and sample preparation dependent[28,29] and therefore careful measurement of both lymphoid tissue and bioengineered synthetic matrices needs to be performed to understand its role in tumor growth. For example, Thomas and colleagues analyzed lymph nodes from B16 melanoma-bearing mice with respect to tumor stage and observed that lymph node metastasis of melanoma was associated with alterations in lymph node extracellular matrix content, increased intranodal pressures and increased lymph node tissue stiffness and viscoelasticity.[28] The technique utilized in this work was indentation methods and yielded values in the range of 100–150 kPa. In contrast, magnetic resonance elastography techniques have reported stiffness of lymphoid tissues in the range of 1.5–3 kPa.[29] Likewise, ultrasound elastography and indentation tests were used to determine mechanical properties of porcine cervical lymph nodes, however stiffness change in abnormal lymph nodes were not determined using these methods.[30] To characterize the mechanical stiffness of lymphoid tissues and apply the same technique to engineered hydrogels, we used a micropipette aspiration method, reported earlier by us.[20,21] This technique quantified the elongation of tissues aspirated inside the pipette in response to applied vacuum pressure (Figure 2A). The strain energy density was chosen as a measure of nonlinear tissue stiffness because prior studies have shown this

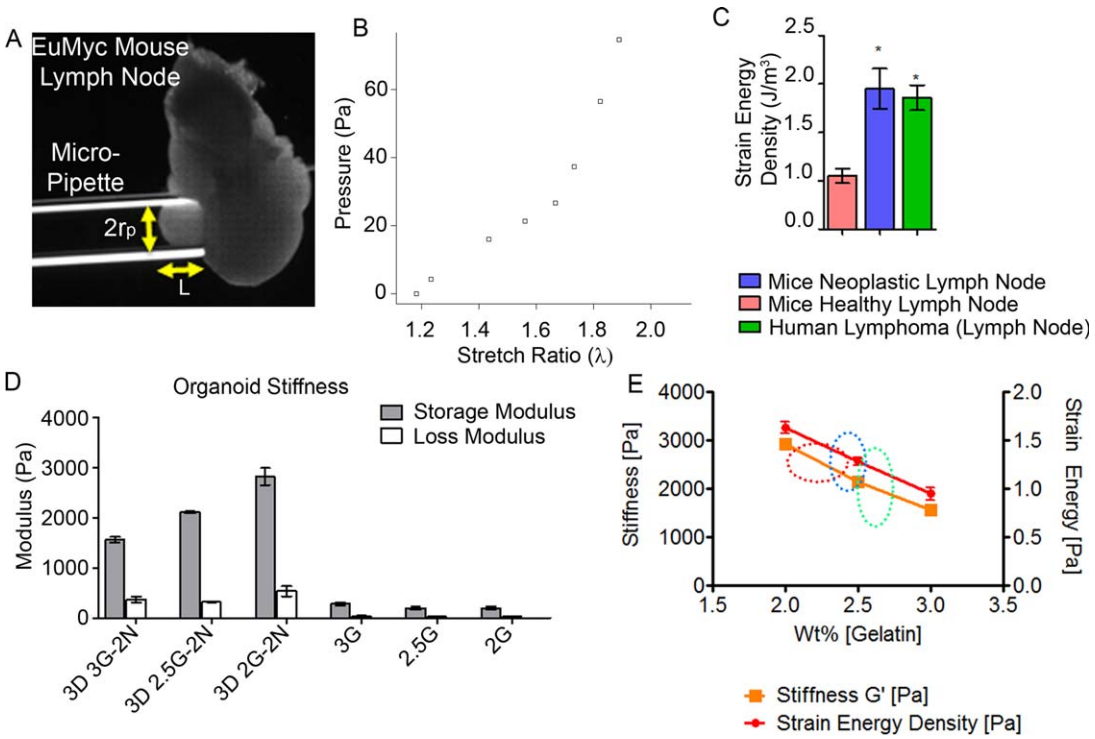


**FIGURE 2**. Mechanical characterization of healthy versus tumorous lymph nodes and spleen, and hydrogel organoids. (A) Photograph showing the mouse tumorous lymph node being aspirated using the micropipette aspiration method. The pipette radius, $r_p$, and the aspirated length, $L$, are indicated. (B) Representative micropipette aspiration data (pressure vs stretch-ratio) for mouse tumorous lymph node. (C) Strain energy density was calculated as the area under pressure (P) vs stretch ratio $\lambda$ curve. Bar graph represents strain energy density (Joules per cubic meter) of healthy and neoplastic lymph nodes from Eμ-myc mice, and a human lymphoid tumor. Lymph node and spleen were freshly isolated from Eμ-myc mice pre-and-post lymphomagenesis. (D) Storage and loss modulus of hydrogels fabricated using gelatin (denoted G) at the indicated concentration (2, 2.5, or 3%) and silicate nanoparticles (denoted N) at a concentration of 2%. (E) Comparison of storage modulus and strain energy density of hydrogel organoid as a function of gelatin weight %. The red oval dotted circle indicates the stiffness range for healthy lymph nodes, blue represents diseased lymph node, and green represents neoplastic splenic tissue stiffness range.

measurement to be less variable for soft tissues than the effective modulus.[20,21] Indeed, attempts to quantify lymphoid tissue stiffness using rheology approaches did not provide meaningful results because the tissue was not fluidic (data not shown). As indicated in Figure 2B,C, the strain energy density for neoplastic mouse lymph node was a significant two-fold higher than the healthy mouse lymph node ($p < 0.5$). We next compared the stiffness of a primary human B-cell lymphoma tissue and observed that the stiffness was comparable to neoplastic mouse tissue ($p > 0.05$). No healthy human lymph node was used in the study because of the unavailability of a healthy donor.

### Biomaterials-based engineered lymphoma organoids with controlled stiffness

Bioengineered *in vitro* models of several cancer types (e.g., melanoma, breast cancer, and lung cancer) have correlated soft or rigid extracellular matrix stiffness with malignant phenotypes.[31,32] These results highlight that stiffness-induced alterations in cell proliferation is dependent on niche and tumor type. Mechanical properties, such as substrate rigidity, have been found to influence the proliferation of human immune cells.[33] However, it remains unknown whether the tissue stiffness of lymph nodes has any effect on lymphomas.

Based on the observations of lymphoid tissue strain energy density, we engineered hydrogel-based lymphoma organoids with strain energy densities in the range of 1–2 J/m$^3$ and coencapsulating lymphomas with supporting human tonsil derived follicular dendritic cells. These hydrogels were engineered by reinforcing gelatin with silicate nanoparticles, a hydrogel platform previously reported by us to support the survival, growth, and differentiation of primary B cells.[22,23] As indicated in Figure 2D, hydrogels fabricated using 2.5% gelatin and reinforced with 2% nanoparticles showed strain energy density comparable to primary human and mouse lymphoma tissue. Although lymphoid tissues could not be analyzed using a rheometer, hydrogel literature has widely reported storage modulus as a stiffness measurement.[22,34–36] We therefore determined the storage and loss modulus of these same set of organoids and observed a similar trend with storage modulus (defined as stiffness hereafter) as was observed with strain energy density, except that the measurement yielded storage modulus values in the range of 1500–3000 Pa (Fig. 2E**)**, which corresponded to 1–2 J/m$^3$ strain energy density using the aspiration method (Fig. 2C**)**. This range of stiffness is similar to values reported for lymphoid tissue stiffness using magnetic resonance elastography.[29] In addition, we have previously reported that gelatin-nanoparticle hydrogels in this

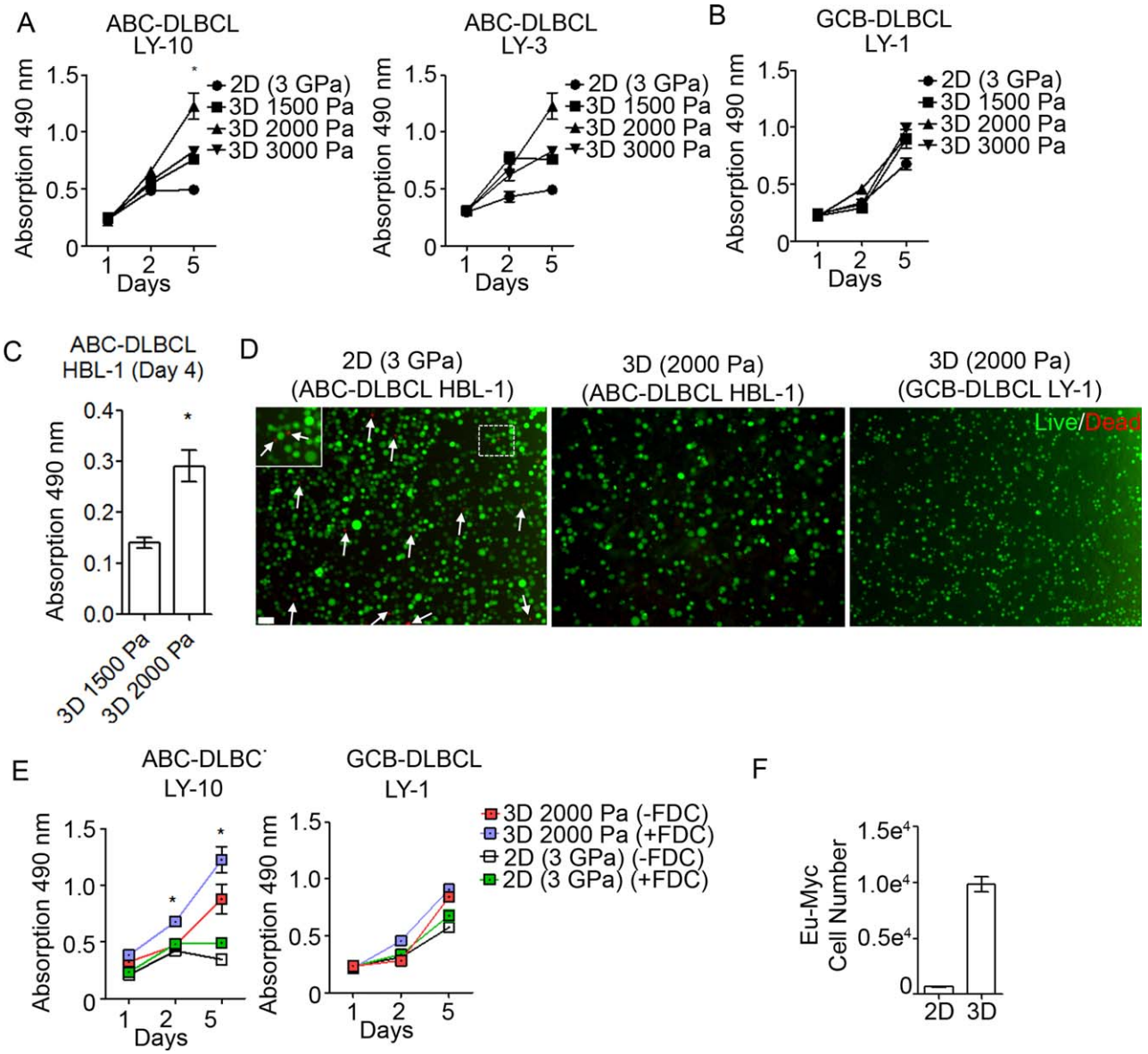


**FIGURE 3**. Lymphoid stiffness regulates proliferation of mature B-cell lymphomas. (A–C) Proliferation of ABC-DLBCL lines (LY-10, LY-3, and HBL-1) and GCB-DLBCL line LY-1 in hydrogel organoids, cocultured with follicular dendritic cells (FDCs). Proliferation was quantified with MTS assay, with FDCs pretreated with mitomycin C (mean ± SEM, $n = 3$, $*p < 0.05$). (D) Fluorescence microscopy projections represent live/dead population of ABC- and GCB-DLBCLs encapsulated within 2000 Pa hydrogels. Images are representative of $n = 3$. Arrows represent dead cells. Scale bar 10 μm. (E) Proliferation of ABC-DLBCL and GCB-DLBCL in 2000 Pa hydrogel organoids, cocultured with or without follicular dendritic cells (FDCs). Proliferation was quantified with MTS assay, with FDCs pretreated with mitomycin C (mean ± SEM, $n = 3$, $*p < 0.05$). (F) Proliferation of primary Eμ-myc lymphomas in 2000 Pa hydrogel organoids or 2D, cocultured with HS-5 bone marrow stromal cells. Proliferation was quantified with MTS assay, with HS-5 cells pretreated with mitomycin C (mean ± SEM, $n = 3$, $*p < 0.05$).

stiffness range support viability and spreading of mammalian cells.[22,23] For the remainder of the studies, this storage modulus (G') was used as a reference for hydrogel organoid stiffness and to study the role of tissue stiffness on lymphoma growth and protein expression levels.

**Organoid stiffness regulate the proliferation of human lymphomas and survival of primary murine lymphomas**

We first determined the role of tissue stiffness on human and mouse lymphoma growth. These studies were performed with and without stromal support. For human lymphomas, follicular dendritic cells (FDCs) were used as a stromal support as reported earlier by us.[17] We hypothesized that the stiffness of lymphoid tissue will modulate the proliferation of lymphoma cells through mechanical stimulation of surface receptors such as integrins and BCR, and possibly through actin-mediated contractility which is known to to be influenced by the extracellular matrix stiffness.[37–39] In these studies, we first examined the role of organoid stiffness on the growth of IgM BCR-dependent ABC-DLBCL cell lines (Fig. 3A) and IgM-BCR independent ABC-DLBCL line OCI-LY3.[40] In both ABC-DLBCL subtypes,

we observed increased growth in all organoids over 5 days of culture and the growth was significantly higher than conventional 2D cultures of lymphoma (Fig. 3A, $p < 0.05$). Importantly, ABC-DLBCLs grown in organoids with medium tissue stiffness (2000 Pa) showed the maximum proliferation as compared to lower stiffness (1500 Pa) and higher stiffness (3000 Pa) organoids. Importantly, the stiffness of the organoid with maximum proliferation was comparable to that of human lymphoma tissue and mouse neoplastic lymph nodes (Figure 2), suggesting that tissue stiffness supports lymphoma growth. When GCB-DLBCL cells, which are IgM-BCR independent, were cultured in the lymphoma organoids, we observed no differences in proliferation rate between 2D and 3D organoid groups (Fig. 3B), suggesting that GCB-DLBCL are either less dependent or independent of lymphoid tissue stiffness. Stiffness-dependent proliferation of ABC-DLBCL was further confirmed with another human ABC-DLBCL line HBL-1 (Fig. 3C), which demonstrated significantly higher proliferation over 4 days of culture in organoids with 2000 Pa stiffness ($p < 0.05$). We observed no differences in survival of ABC or GCB-DLBCLs in 3D organoids as compared to 2D cultures, as indicated by live dead staining in Figure 3D. These studies further highlight an important observation that there exists an optimum tissue stiffness at which lymphomas proliferate, which is distinct from the observations with tumors of non-lymphoid origin such as mammary tumors where increasing stiffness correlates with tumor growth.[12] The reasons for these observations are not entirely clear and may be dependent on other phenotypic changes in these cells. Therefore, future *ex vivo* and *in vivo* studies are needed to understand the mechanism behind lower proliferation in 3000 Pa organoids.

We next determined the role of FDCs on the growth of ABC-DLBCL and GCB-DLBCL in organoids with similar mechanical stiffness to patient tissue. In ABC-DLBCL, presence of growth-arrested FDCs supported significantly higher lymphoma proliferation as compared to organoids that did not contain follicular dendritic cells (Fig. 3E, $p < 0.05$). These differences were not observed in 2D cocultures. Unlike ABC-DLBCLs, GCB-DLBCLs did not show any significant differences between organoids and 2D cultures, with or without FDCs (Fig. 3D). These studies further indicate that GCB-DLBCLs are less dependent on lymphoid tumor microenvironment than ABC-DLBCL.

We next determined the role of 2000 Pa hydrogel stiffness on the survival of primary Eμ-myc lymphomas in organoids as compared to 2D cocultures. Previous studies have shown that bone marrow stromal cells are critical for the survival of primary Eμ-myc lymphomas.[41] We screened HS-5 bone marrow stromal cells which sustain hematopoiesis,[42–44] our previously reported 40LB stromal cells that present mouse CD40 Ligand and B-cell activating factors,[22,23,45] JAWSII mouse dendritic cells,[46,47] and human follicular dendritic cells HK[16,17] for sustaining the short term survival of primary Eμ-myc lymphomas. Only HS-5 sustained the survival of primary Eμ-myc lymphomas (data not shown) and therefore we used HS-5 stromal cells in 3D

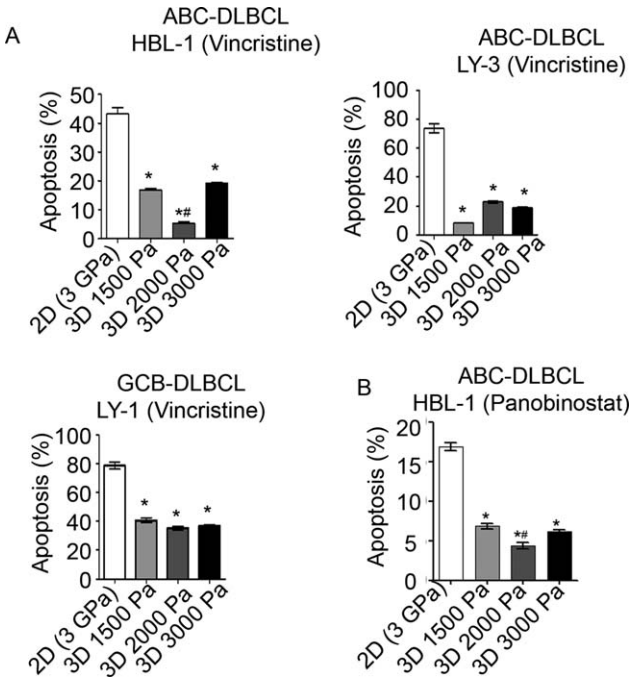


**FIGURE 4**. Lymphoid tissue stiffness modulates drug resistance in mature B-cell lymphomas treated with the conventional chemotherapy drug vincristine or histone deacetylase inhibitor Panobinostat. (A) Bar graphs represent % apoptosis in B-cell lymphomas exposed to vincristine. ABC-DLBCL cell lines HBL-1 and LY-3, and GCB-DLBCL cell line LY-1 were cultured for 3 days in 2D or 3D organoids and exposed to 1 m*M* vincristine for 48 hours. B-cell lymphomas were stained with APC-IgM BCR and Annexin V-FITC for apoptosis analysis (mean ± SEM, $n = 3$, $^{*}p < 0.05$ compared to all 3D groups and $^{\#}p < 0.05$ compared to all other 3D groups). (B) Bar graphs represent % apoptosis in IgM BCR dependent ABC-DLBCL line HBL-1 exposed to HDACi Panobinostat. HBL-1 was cultured for 3 days in 2D cultures or 3D organoids and exposed to 50 nM Panobinostat for 24 hours. B-cell lymphoma cells were stained with CD19 and Annexin V-FITC for apoptosis analysis (mean ± SEM, $n = 3$, $^{*}p < 0.05$ compared to all 3D groups and $^{\#}p < 0.05$ compared to all other 3D and 2D groups).

organoids. As indicated in Figure 3F, 2000 Pa hydrogel stiffness resulted in significantly higher survival of Eμ-myc cells as compared to 2D cells ($p < 0.05$). These findings suggest that matching the appropriate soft tissue stiffness and supporting stromal cells is important for prolonging the survival and growth of primary and established lymphomas.

### Stiffness promotes drug resistance against standard chemotherapy and Histone Deacetylase inhibitor

Since most studies to date have focused on drug-lymphoma interactions under 2D conditions, we hypothesized that increased proliferation under the effect of lymphoid tissue stiffness will reduce the apoptosis of ABC-DLBCLs when exposed to anti-lymphoma drugs. In separate experiments, we exposed ABC- and GCB-DLBCLs to either the conventional chemotherapy drug vincristine or a Histone Deacetylase inhibitor (HDACi) Panobinostat. Histone acetylation or histone deacetylation processes play key roles in the epigenetic regulation of cells. HDACi are a new class of drugs that have shown promise in early-phase clinical trials for the treatment of hematological malignancies. For example,

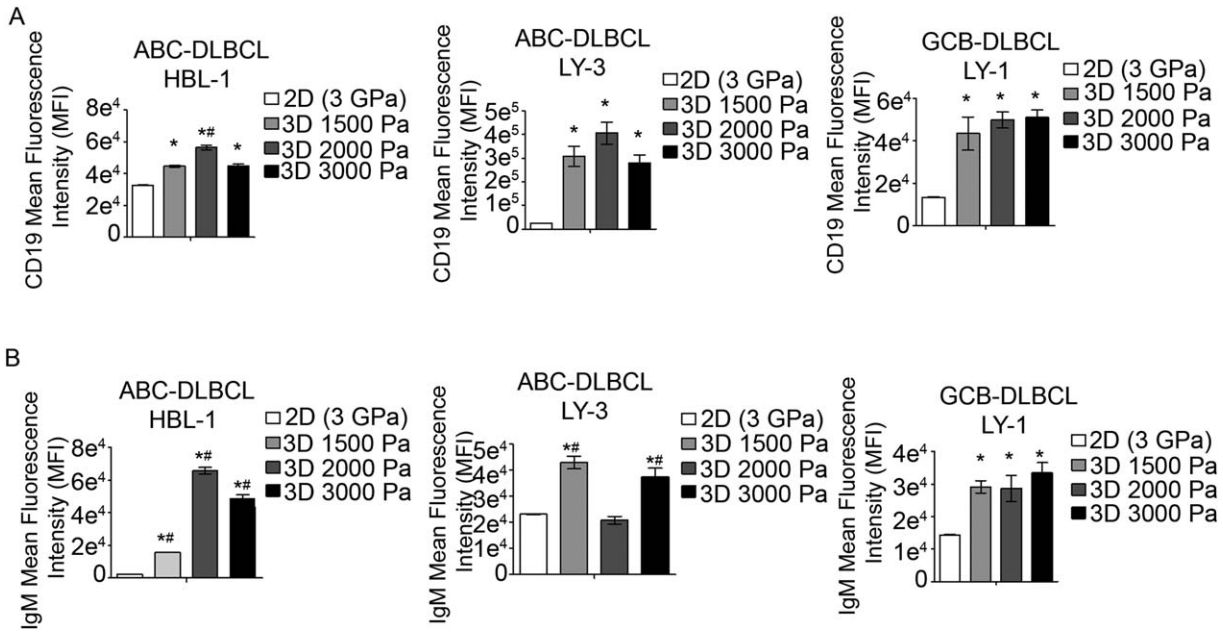


**FIGURE 5**. Effect of lymphoid tissue stiffness on B-cell lymphoma markers and B-cell receptor. (A and B) Bar graphs represent flow cytometry analysis (mean fluorescence intensity (MFI)) of (A) CD19 and (B) IgM surface markers in ABC- and GCB-DLBCL cells cultured in 2D condition or 3D organoids (all with FDCs) (mean ± SEM, $n = 3$, $^{*}p < 0.05$, ANOVA and $^{\#}p < 0.05$ compared to all other 3D groups).

in a phase II B study,[48] 24% of refractory cutaneous T-cell lymphoma (CTCL) patients who had originally failed conventional therapies had a complete or partial response to vorinostat, an FDA approved HDACi. Another drug of interest is Panobinostat that has been tested in hematological malignancies such as acute myeloid leukemia (AML)[49] and multiple myeloma.[50,51] We have previously shown that Panobinostat induces less apoptosis in lymphomas when they are treated with the drug in a tumor-specific microenvironment, such as in the presence of pro-survival integrin binding ligands[17]; however, not much is known about the drug response in B-cell lymphomas in the context of tissue stiffness.

As indicated in Figure 4A,B, when exposed to either vincristine of Panobinostat, a significant 20–40% lower Annexin-V staining (apoptosis) was observed in HBL-1 cells grown in 3D organoids of varying stiffness as compared to 2D growth conditions. Organoids with tissue stiffness (2000 Pa) comparable to human lymphoma tissue stiffness demonstrated maximum resistance to apoptosis within organoid groups (resistance: 1500 < 2000 > 3000 Pa). Since HBL-1 is IgM BCR-dependent ABC-DLBCL, we further determined the effect of these drugs on a BCR-independent ABC-DLBCL to better understand the relationship between drug response and BCR signaling. Unlike HBL-1 ABC-DLBCLs, BCR independent LY3 showed the lowest apoptosis in the softest organoids instead of an organoid with intermediate stiffness, although all organoids demonstrated significant lower apoptosis than in 2D growth conditions (resistance: 1500 > 2000 Pa = 3000 Pa). Similar to ABC-DLBCLs, we observed reduced apoptosis in GCB-DLBCL OCI-LY1 cells grown in 3D organoids; however we did not observe any difference in drug resistance between the soft and stiff organoids.

These observations support the proliferation results where ABC-DLBCL proliferation was dependent on organoid stiffness, whereas GCB-DLBCL proliferation was independent of stiffness. We do not anticipate drug diffusion to be responsible for these differences because these organoids have been previously used for cytokine delivery and antibody staining.[22] The general reduction in apoptosis observed in 3D microenvironment as compared to classic 2D cultures are consistent with our previous reported work, where similar drug uptake was observed under both 3D and 2D conditions.[17] Instead, we hypothesize that reduced apoptosis in the 3D organoid microenvironment can be attributed to differential regulation of pro-survival signals such as integrin receptors and BCR on these cells. To test this hypothesis, we evaluated the expression level of hallmark markers CD19 and BCR on the surface of cells either grown in 2D or in 3D organoids with varying stiffness. As indicated in Figure 5A, IgM-dependent ABC-DLBCL (HBL-1) upregulated the expression level of CD19 in 3D organoids as compared to 2D cultures, and maximum CD19 expression level was observed at 2000 Pa stiffness. Similar observations were made with IgM-independent ABC-DLBCL cell line LY-3. In contrast, while GCB-DLBCL upregulated the expression of CD19 in 3D, no differences were observed among the three hydrogel stiffness values that were studied. Importantly, IgM BCR expression was highly dependent on stiffness in ABC-DLBCL (Fig. 5B**)**. In HBL-1 ABC-DLBCLs, 2000 Pa stiff hydrogels demonstrated maximum upregulation of IgM-BCR whereas in LY-3, 2000 Pa stiffness significantly reduced IgM expression level between the three organoid stiffness. There was no effect of stiffness in LY-1 GCB-DLBCL, and all 2D cultures had lower expression levels of IgM-BCR.

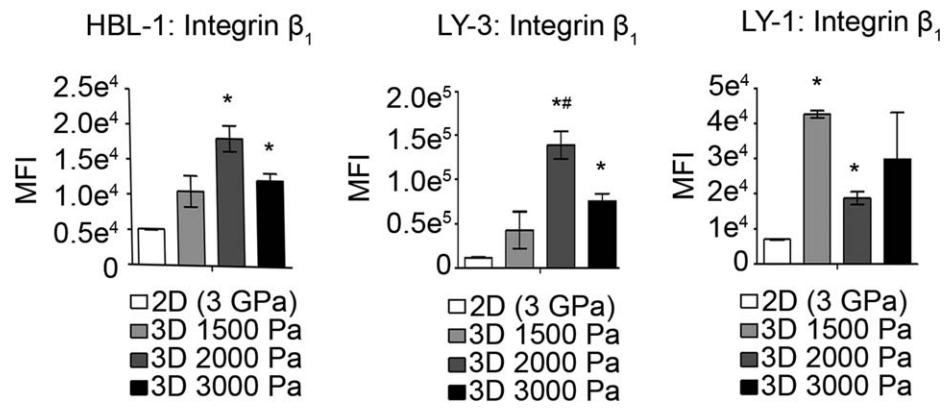


**FIGURE 6**. Lymphoid tissue stiffness differentially regulates the integrin β1 expression in genetically diverse B-cell lymphomas. Bar graphs represent flow cytometry analysis [mean fluorescence intensity (MFI)] of integrin β1 surface markers in ABC- and GCB-DLBCL cells cultured in 2D condition or 3D organoids (all with FDCs) (mean ± SEM, $n = 3$, $^{*}p < 0.05$, ANOVA and $^{\#}p < 0.05$ compared to all other 3D groups).

This observation is important because in ABC-DLBCLs, IgM BCR is chronically activated and has implications in lymphoma survival and progression.[1,52] The BCR is a transmembrane protein complex located on the outer surface of healthy and malignant B cells.[52] It is a heterodimer composed of heavy-chain and light-chain immunoglobulins (Igs), CD79A/Igα, and CD79B/Igβ. ABC-DLBCLs are commonly associated with mutations of components in the BCR pathway, such as CD79A/B (~20% of ABC-DLBCLs),[5] CARD11 (~10%),[6] and several others. Targeting hallmark pathways of ABC-DLBCL, such as those activated by the BCR, has the potential to impact a broad cross-section of ABC-DLBCL patients.[53,54]

Proposed therapeutic strategies for ABC-DLBCL target proteins that signal downstream of the BCR pathway, including kinase inhibitors targeting Bruton's tyrosine kinase (BTK), mitogen-activated protein kinases (MAPKs), and AKT.[1] These signaling mediators intersect with integrins such as α4β1, and other mechano-transduction pathways,[55–57] which can be activated through adhesion to extracellular matrix and tissue stiffness. Therefore, we next determined the expression level of integrin β1 in human lymphomas and primary mouse lymphomas. As indicated in Figure 6, integrin β1 mean fluorescent intensity was significantly higher in 2000 Pa organoids in both IgM-dependent and –independent ABC-DLBCLs ($p < 0.05$). In contrast, expression level of integrin b1 in GCB-DLBCL was higher in the softest organoid (1500 Pa) and not in intermediate 2000 Pa organoids. Since previous studies have shown that integrin β1 supports survival and growth of ABC-DLBCLs, this current study suggests that the stiffness of lymphoid tissue can upregulate the expression level of mechanoreceptor integrin β1 in *ex vivo* cultures. We further observed an increase in integrin β1 expression in primary Eμ-Myc lymphomas as well, as compared to 2D cocultures, a finding that supports the need for modular 3D lymphoma tissue constructs with tunable stiffness for supporting primary and established lymphoma cultures. We used the 2000 Pa stiffness to compare differences in expression levels of IgM BCR in primary lymphoma tissues when cultured in 3D versus 2D conditions. We cultured Eμ-Myc tumors with HS-5 in 2D cocultures and 3D organoids, and observed a significant increase in IgM-BCR levels (Figure 7), which suggested that 3D organoids modulated the expression levels of surface markers in primary mouse tumors.

Stiffness and deformation of extra cellular matrix are strongly regulated by actomyosin contractility.[39] Because

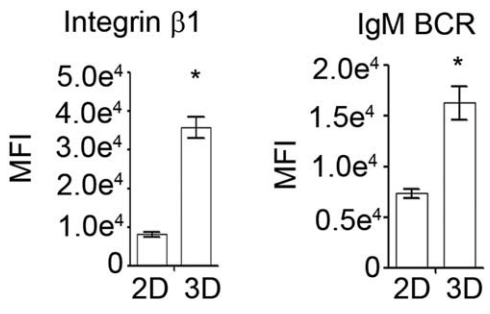


**FIGURE 7**. Effect of lymphoid tissue stiffness on integrin β1 and IgM BCR expression in primary mouse B-cell lymphomas. Bar graphs represent flow cytometry analysis [mean fluorescence intensity (MFI)] of integrin β1 and IgM BCR surface markers in primary Eμ-myc lymphomas cultured in 2D condition or 3D organoids (all with HS-5) (mean ± SEM, $n = 3$, $^{*}p < 0.05$, *t* test).

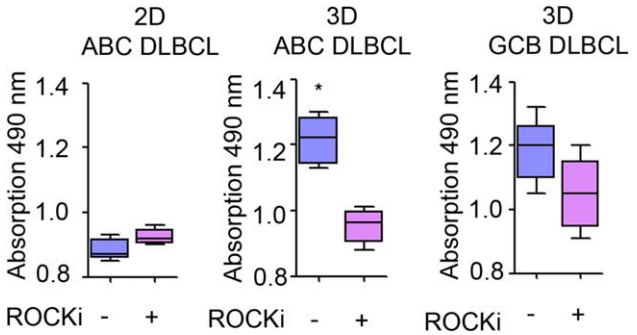


**FIGURE 8**. Lymphoid tissue stiffness modulates actomyosin contractility in human B-cell lymphomas. Bar graphs represent cell proliferation analysis of ABC-DLBCL or GCB-DLBCL cells cultured in 2D conditions or 3D organoids, in the absence or presence of ROCKi (all with follicular dendritic cells) (mean ± SEM, $n = 3$, $^{*}p < 0.05$, *t* test).

our results indicated that the expression levels of integrin β1 in lymphomas were regulated by matrix stiffness and since previous studies have shown that integrin β1 is linked to the actin cytoskeleton via association with proteins such as talin and vinculin,[58–60] we hypothesized that the enhanced growth of lymphomas in 2000 Pa organoids could be attributed to integrin-actin-mediated contractility. We therefore inhibited actin-myosin contractility using a Rho-ROCK inhibitor (Y-27632).[55,61] As indicated in Figure 8, inhibiting contractility did not affect ABC-DLBCLs in 2D cultures, but significantly reduced proliferation in 2000 Pa 3D organoids. This effect was not observed in GCB-DLBCL, which suggested that contractility mediated proliferation was specific to ABC-DLBCL.

## CONCLUSION

Our results are the first evidence that lymphoma survival, proliferation, drug response, and BCR signaling is influenced by lymphoid tissue stiffness in a molecular subtype dependent manner. These results emphasize the role of tumor stiffness matched biomaterial organoids and lymphoid tissue stiffness in progression and drug response of malignant B-cell tumors. In the past, lymphoid tissue stiffness and mechanosensing has been largely ignored in mechanistic study of lymphoma progression and its therapeutic evaluation of B-cell lymphomas *ex vivo*. Therefore, investigation of chemotherapeutics and upcoming new classes of therapeutic agents that target epigenetic, matrix, or angiogenesis pathways should consider the potential confounding interactions between the lymphoid tumor microenvironment and cell-molecular level. Future studies will determine the independent role of tissue bioadhesive signals, stiffness,[10,36] and stress relaxation[62] in the proliferation and drug response in lymphomas and may require modular biomaterials with controlled presentation of these biophysical stimuli.[63,64]


## ACKNOWLEDGMENTS

The authors thank Dr. Jude Phillip at Weill Cornell Medical College of Cornell University for handling primary human lymphoma tissue and Yashira Negron Abril for assistance with Eμ-Myc mouse genotyping. The content is solely the responsibility of the authors and does not necessarily represent the official views of the funding agencies.


## REFERENCES


1. Fontan L, Melnick A. Molecular pathways: targeting MALT1 paracaspase activity in lymphoma, Clin Cancer Res 2013;19: 6662–8.
2. Fontan L, Yang C, Kabaleeswaran V, Volpon L, Osborne MJ, Beltran E, Garcia M, Cerchietti L, Shaknovich R, Yang SN, Fang F, Gascoyne RD, Martinez-Climent JA, Glickman JF, Borden K, Wu H, Melnick A. MALT1 small molecule inhibitors specifically suppress ABC-DLBCL in vitro and in vivo, Cancer Cell 2012;22: 812–24.
3. Alizadeh AA, Eisen MB, Davis RE, Ma C, Lossos IS, Rosenwald A, Boldrick JC, Sabet H, Tran T, Yu X, Powell JI, Yang L, Marti GE, Moore T, Hudson J, Jr., Lu L, Lewis DB, Tibshirani R, Sherlock G, Chan WC, Greiner TC, Weisenburger DD, Armitage JO, Warnke R, Levy R, Wilson W, Grever MR, Byrd JC, Botstein D, Brown PO, Staudt LM. Distinct types of diffuse large B-cell lymphoma identified by gene expression profiling, Nature 2000;403:503–11.
4. Davis RE, Brown KD, Siebenlist U, Staudt LM. Constitutive nuclear factor kappaB activity is required for survival of activated B cell-like diffuse large B cell lymphoma cells, J Exp Med 2001;194: 1861–74.
5. Davis RE, Ngo VN, Lenz G, Tolar P, Young RM, Romesser PB, Kohlhammer H, Lamy L, Zhao H, Yang Y, Xu W, Shaffer AL, Wright G, Xiao W, Powell J, Jiang JK, Thomas CJ, Rosenwald A, Ott G, Muller-Hermelink HK, Gascoyne RD, Connors JM, Johnson NA, Rimsza LM, Campo E, Jaffe ES, Wilson WH, Delabie J, Smeland EB, Fisher RI, Braziel RM, Tubbs RR, Cook JR, Weisenburger DD, Chan WC, Pierce SK, Staudt LM. Chronic active B-cell-receptor signalling in diffuse large B-cell lymphoma, Nature 2010;463:88–92.
6. Lenz G, Davis RE, Ngo VN, Lam L, George TC, Wright GW, Dave SS, Zhao H, Xu W, Rosenwald A, Ott G, Muller-Hermelink HK, Gascoyne RD, Connors JM, Rimsza LM, Campo E, Jaffe ES, Delabie J, Smeland EB, Fisher RI, Chan WC, Staudt LM. Oncogenic CARD11 mutations in human diffuse large B cell lymphoma, Science 2008;319:1676–9.
7. Lenz G, Wright G, Dave SS, Xiao W, Powell J, Zhao H, Xu W, Tan B, Goldschmidt N, Iqbal J, Vose J, Bast M, Fu K, Weisenburger DD, Greiner TC, Armitage JO, Kyle A, May L, Gascoyne RD, Connors JM, Troen G, Holte H, Kvaloy S, Dierickx D, Verhoef G, Delabie J, Smeland EB, Jares P, Martinez A, Lopez-Guillermo A, Montserrat E, Campo E, Braziel RM, Miller TP, Rimsza LM, Cook JR, Pohlman B, Sweetenham J, Tubbs RR, Fisher RI, Hartmann E, Rosenwald A, Ott G, Muller-Hermelink HK, Wrench D, Lister TA, Jaffe ES, Wilson WH, Chan WC, Staudt LM, Lymphoma P/Leukemia Molecular Profiling. Stromal gene signatures in large-B-cell lymphomas, N Engl J Med 2008;359:2313–23.
8. Roschewski M, Staudt LM, Wilson WH. Diffuse large B-cell lymphoma-treatment approaches in the molecular era, Nat Rev Clin Oncol 2014;11:12–23.
9. Sehn LH, Gascoyne RD. Diffuse large B-cell lymphoma: optimizing outcome in the context of clinical and biologic heterogeneity, Blood 2015;125:22–32.
10. Chaudhuri O, Koshy ST, Branco da Cunha C, Shin JW, Verbeke CS, Allison KH, Mooney DJ. Extracellular matrix stiffness and composition jointly regulate the induction of malignant phenotypes in mammary epithelium, Nat Mater 2014;13:970–8.
11. Paszek MJ, DuFort CC, Rossier O, Bainer R, Mouw JK, Godula K, Hudak JE, Lakins JN, Wijekoon AC, Cassereau L, Rubashkin MG, Magbanua MJ, Thorn KS, Davidson MW, Rugo HS, Park JW, Hammer DA, Giannone G, Bertozzi CR, Weaver VM. The cancer glycocalyx mechanically primes integrin-mediated growth and survival, Nature 2014;511:319–25.
12. Paszek MJ, Zahir N, Johnson KR, Lakins JN, Rozenberg GI, Gefen A, Reinhart-King CA, Margulies SS, Dembo M, Boettiger D, Hammer DA, Weaver VM. Tensional homeostasis and the malignant phenotype, Cancer Cell 2005;8:241–54.
13. Scott DW, Gascoyne RD. The tumour microenvironment in B cell lymphomas, Nat Rev Cancer 2014;14:517–34.
14. Damiano JS, Dalton WS. Integrin-mediated drug resistance in multiple myeloma, Leuk Lymphoma 2000;38:71–81.
15. Naci D, El Azreq MA, Chetoui N, Lauden L, Sigaux F, Charron D, Al-Daccak R, Aoudjit F. alpha2beta1 integrin promotes chemoresistance against doxorubicin in cancer cells through extracellular signal-regulated kinase (ERK), J Biol Chem 2012;287:17065–76.
16. Cayrol F, Diaz Flaque MC, Fernando T, Yang SN, Sterle HA, Bolontrade M, Amoros M, Isse B, Farias RN, Ahn H, Tian YF, Tabbo F, Singh A, Inghirami G, Cerchietti L, Cremaschi GA. Integrin alphavbeta3 acting as membrane receptor for thyroid hormones mediates angiogenesis in malignant T cells, Blood 2015;125:841–51.
17. Tian YF, Ahn H, Schneider RS, Yang SN, Roman-Gonzalez L, Melnick AM, Cerchietti L, Singh A. Integrin-specific hydrogels as adaptable tumor organoids for malignant B and T cells, Biomaterials 2015;73:110–119.
18. Seo BR, Bhardwaj P, Choi S, Gonzalez J, Andresen Eguiluz RC, Wang K, Mohanan S, Morris PG, Du B, Zhou XK, Vahdat LT, Verma A, Elemento O, Hudis CA, Williams RM, Gourdon D, Dannenberg AJ, Fischbach C. Obesity-dependent changes in interstitial ECM mechanics promote breast tumorigenesis, Sci Transl Med 2015;7:301ra130.

19. Shin JW, Mooney DJ. Extracellular matrix stiffness causes systematic variations in proliferation and chemosensitivity in myeloid leukemias, Proc Natl Acad Sci U S A 2016;113:12126–12131.
20. Buskohl PR, Gould RA, Butcher JT. Quantification of embryonic atrioventricular valve biomechanics during morphogenesis, Journal of biomechanics 2012;45:895–902.
21. Buskohl PR, Sun MJ, Thompson RP, Butcher JT. Serotonin potentiates transforming growth factor-beta3 induced biomechanical remodeling in avian embryonic atrioventricular valves, PLoS One 2012;7:e42527.
22. Purwada A, Jaiswal MK, Ahn H, Nojima T, Kitamura D, Gaharwar AK, Cerchietti L, Singh A. Ex vivo engineered immune organoids for controlled germinal center reactions, Biomaterials 2015;63: 24–34.
23. Purwada A, Singh A. Immuno-engineered Organoids for Regulating the Kinetics of B cell Development and Antibody Production, Nature Protocols 2017;12:168–182.
24. Butcher JT, McQuinn TC, Sedmera D, Turner D, Markwald RR. Transitions in early embryonic atrioventricular valvular function correspond with changes in cushion biomechanics that are predictable by tissue composition, Circ Res 2007;100:1503–11.
25. Singh A, Qin H, Fernandez I, Wei J, Lin J, Kwak LW, Roy K. An injectable synthetic immune-priming center mediates efficient T-cell class switching and T-helper 1 response against B cell lymphoma, Journal of controlled release : official journal of the Controlled Release Society 2011;155:184–92.
26. Singh A, Nie H, Ghosn B, Qin H, Kwak LW, Roy K. Efficient modulation of T-cell response by dual-mode, single-carrier delivery of cytokine-targeted siRNA and DNA vaccine to antigen-presenting cells, Mol Ther 2008;16:2011–21.
27. Harris AW, Pinkert CA, Crawford M, Langdon WY, Brinster RL, Adams JM. The E mu-myc transgenic mouse. A model for high-incidence spontaneous lymphoma and leukemia of early B cells, J Exp Med 1988;167:353–71.
28. Rohner NA, McClain J, Tuell SL, Warner A, Smith B, Yun Y, Mohan A, Sushnitha M, Thomas SN. Lymph node biophysical remodeling is associated with melanoma lymphatic drainage, FASEB J 2015;29:4512–22.
29. Hirsch S, Guo J, Reiter R, Papazoglou S, Kroencke T, Braun J, Sack I. MR elastography of the liver and the spleen using a piezoelectric driver, single-shot wave-field acquisition, and multifrequency dual parameter reconstruction, Magn Reson Med 2014;71: 267–77.
30. Wing-Han Yuen Q, Zheng YP, Huang YP, He JF, Chung-Wai Cheung J, Ying M. In-vitro Strain and Modulus Measurements in Porcine Cervical Lymph Nodes, Open Biomed Eng J 2011;5:39–46.
31. Tan Y, Tajik A, Chen J, Jia Q, Chowdhury F, Wang L, Zhang S, Hong Y, Yi H, Wu DC, Zhang Y, Wei F, Poh YC, Seong J, Singh R, Lin LJ, Doganay S, Li Y, Jia H, Ha T, Wang Y, Huang B, Wang N. Matrix softness regulates plasticity of tumour-repopulating cells via H3K9 demethylation and Sox2 expression, Nat Commun 2014; 5:4619.
32. Tilghman RW, Cowan CR, Mih JD, Koryakina Y, Gioeli D, Slack-Davis JK, Blackman BR, Tschumperlin DJ, Parsons JT. Matrix rigidity regulates cancer cell growth and cellular phenotype, PLoS One 2010;5:e12905.
33. O'Connor RS, Hao X, Shen K, Bashour K, Akimova T, Hancock WW, Kam LC, Milone MC. Substrate rigidity regulates human T cell activation and proliferation, J Immunol 2012;189:1330-9.
34. Yan C, Pochan DJ. Rheological properties of peptide-based hydrogels for biomedical and other applications, Chemical Society reviews 2010;39:3528–40.
35. Hutson CB, Nichol JW, Aubin H, Bae H, Yamanlar S, Al-Haque S, Koshy ST, Khademhosseini A. Synthesis and characterization of tunable poly(ethylene glycol): gelatin methacrylate composite hydrogels, Tissue Eng Part A 2011;17:1713–23.
36. Patel RG, Purwada A, Cerchietti L, Inghirami G, Melnick A, Gaharwar AK, Singh A. Microscale Bioadhesive Hydrogel Arrays for Cell Engineering Applications, Cell Mol Bioeng 2014;7: 394–408.
37. Reichl EM, Ren Y, Morphew MK, Delannoy M, Effler JC, Girard KD, Divi S, Iglesias PA, Kuo SC, Robinson DN. Interactions between myosin and actin crosslinkers control cytokinesis contractility dynamics and mechanics, Curr Biol 2008;18:471–80.
38. Butcher DT, Alliston T, Weaver VM. A tense situation: forcing tumour progression, Nat Rev Cancer 2009;9:108–22.
39. Swaminathan V, Mythreye K, O'Brien ET, Berchuck A, Blobe GC, Superfine R. Mechanical stiffness grades metastatic potential in patient tumor cells and in cancer cell lines, Cancer Res 2011;71: 5075–80.
40. Clozel S.Y. T, Elstrom R, Tam W, Martin P, Kormaksson M, Banerjee S, Vasanthakumar A, Culjkovic B, Scott D, Brennan S, Leser M, Shaknovich R, Chadburn A, Tabbo F, Godley L, Gascoyne R, Borden K, Inghirami G, Leonard J, Melnick A, Cerchietti L. Mechanism-Based Epigenetic Chemosensitization Therapy of Diffuse Large B Cell Lymphoma, Cancer Discovery 2013;3:1002–19.
41. Dierks C, Grbic J, Zirlik K, Beigi R, Englund NP, Guo GR, Veelken H, Engelhardt M, Mertelsmann R, Kelleher JF, Schultz P, Warmuth M. Essential role of stromally induced hedgehog signaling in B-cell malignancies, Nat Med 2007;13:944–51.
42. Roecklein BA, Torok-Storb B. Functionally distinct human marrow stromal cell lines immortalized by transduction with the human papilloma virus E6/E7 genes, Blood 1995;85:997-1005.
43. Graf L, Iwata M, Torok-Storb B. Gene expression profiling of the functionally distinct human bone marrow stromal cell lines HS-5 and HS-27a, Blood 2002;100:1509–11.
44. Mhyre AJ, Marcondes AM, Spaulding EY, Deeg HJ. Stroma-dependent apoptosis in clonal hematopoietic precursors correlates with expression of PYCARD, Blood 2009;113;649–58.
45. Nojima T, Haniuda K, Moutai T, Matsudaira M, Mizokawa S, Shiratori I, Azuma T, Kitamura D. In-vitro derived germinal centre B cells differentially generate memory B or plasma cells in vivo, Nat Commun 2011;2:465.
46. Purwada A, Tian YF, Huang WS, Rohrbach KM, Deol S, August A, Singh A. Self-Assembly Protein Nanogels for Safer Cancer Immunotherapy, Adv Healthc Mater 2016;5:1413–1419.
47. Ali OA, Huebsch N, Cao L, Dranoff G, Mooney DJ. Infection-mimicking materials to program dendritic cells in situ, Nat Mater 2009;8:151–8.
48. Duvic M, Vu J. Update on the treatment of cutaneous T-cell lymphoma (CTCL): Focus on vorinostat, Biologics 2007;1:377–92.
49. Mandawat A, Fiskus W, Buckley KM, Robbins K, Rao R, Balusu R, Navenot JM, Wang ZX, Ustun C, Chong DG, Atadja P, Fujii N, Peiper SC, Bhalla K. Pan-histone deacetylase inhibitor panobinostat depletes CXCR4 levels and signaling and exerts synergistic antimyeloid activity in combination with CXCR4 antagonists, Blood 2010;116:5306–15.
50. San-Miguel JF, Hungria VT, Yoon SS, Beksac M, Dimopoulos MA, Elghandour A, Jedrzejczak WW, Gunther A, Nakorn TN, Siritanaratkul N, Corradini P, Chuncharunee S, Lee JJ, Schlossman RL, Shelekhova T, Yong K, Tan D, Numbenjapon T, Cavenagh JD, Hou J, LeBlanc R, Nahi H, Qiu L, Salwender H, Pulini S, Moreau P, Warzocha K, White D, Blade J, Chen W, Gimsing J de la Rubia, P, Lonial S, Kaufman JL, Ocio EM, Veskovski L, Sohn SK, Wang MC, Lee JH, Einsele H, Sopala M, Corrado C, Bengoudifa BR, Binlich F, Richardson PG. Panobinostat plus bortezomib and dexamethasone versus placebo plus bortezomib and dexamethasone in patients with relapsed or relapsed and refractory multiple myeloma: a multicentre, randomised, double-blind phase 3 trial, Lancet Oncol 2014;15:1195–206.
51. Richardson PG, Schlossman RL, Alsina M, Weber DM, Coutre SE, Gasparetto C, Mukhopadhyay S, Ondovik MS, Khan M, Paley CS, Lonial S. PANORAMA 2: panobinostat in combination with bortezomib and dexamethasone in patients with relapsed and bortezomib-refractory myeloma, Blood 2013;122:2331–7.
52. Kuppers R. Mechanisms of B-cell lymphoma pathogenesis, Nat Rev Cancer 2005;5:251-62.
53. Brower V. Ibrutinib promising in subtype of DLBCL, Lancet Oncol 2015;16:e428.
54. Wilson WH, Young RM, Schmitz R, Yang Y, Pittaluga S, Wright G, Lih CJ, Williams PM, Shaffer AL, Gerecitano J, Goy S de Vos, A, Kenkre VP, Barr PM, Blum KA, Shustov A, Advani R, Fowler NH, Vose JM, Elstrom RL, Habermann TM, Barrientos JC, McGreivy J, Fardis M, Chang BY, Clow F, Munneke B, Moussa D, Beaupre DM,

Staudt LM. Targeting B cell receptor signaling with ibrutinib in diffuse large B cell lymphoma, Nature medicine 2015;21:922–6.
55. Dumbauld DW, Lee TT, Singh A, Scrimgeour J, Gersbach CA, Zamir EA, Fu J, Chen CS, Curtis JE, Craig SW, Garcia AJ. How vinculin regulates force transmission, Proc Natl Acad Sci U S A 2013;110:9788–93.
56. Singh A, Suri S, Lee T, Chilton JM, Cooke MT, Chen W, Fu J, Stice SL, Lu H, McDevitt TC, Garcia AJ. Adhesion strength-based, label-free isolation of human pluripotent stem cells, Nat Methods 2013; 10:438–44.
57. Puklin-Faucher E, Sheetz MP. The mechanical integrin cycle, J Cell Sci 2009;122:179–86.
58. Brakebusch C, Wennerberg K, Krell HW, Weidle UH, Sallmyr A, Johansson S, Fassler R. Beta1 integrin promotes but is not essential for metastasis of ras-myc transformed fibroblasts, Oncogene 1999;18:3852–61.
59. Lahlou H, Muller WJ. beta1-integrins signaling and mammary tumor progression in transgenic mouse models: implications for human breast cancer, Breast cancer research : BCR 2011;13:229.
60. Michael KE, Garcia AJ. Cell adhesion strengthening: measurement and analysis, Methods Cell Biol 2007;83:329–46.
61. Coyer SR, Singh A, Dumbauld DW, Calderwood DA, Craig SW, Delamarche E, Garcia AJ. Nanopatterning reveals an ECM area threshold for focal adhesion assembly and force transmission that is regulated by integrin activation and cytoskeleton tension, J Cell Sci 2012;125:5110–5123.
62. Chaudhuri O, Gu L, Klumpers D, Darnell M, Bencherif SA, Weaver JC, Huebsch N, Lee HP, Lippens E, Duda GN, Mooney DJ. Hydrogels with tunable stress relaxation regulate stem cell fate and activity, Nat Mater 2016;15:326-34.
63. Purwada A, Shah SB, Beguelin W, Melnick A, Singh A. Modular Immune Organoids with Integrin Ligand Specificity Differentially Regulate Ex vivo B Cell Activation, ACS Biomater. Sci. Eng. 2017; 3:214–225.
64. Lee TT, Garcia JR, Paez JI, Singh A, Phelps EA, Weis S, Shafiq Z, Shekaran A, Del Campo A, Garcia AJ. Light-triggered in vivo activation of adhesive peptides regulates cell adhesion, inflammation and vascularization of biomaterials, Nature materials 2015;14:352-60.